NASA CONTRACTOR
REPORT

NASA CR-149977

(NASA-CR-149977) EXPERIMENTAL DEVELOPMENT OF PROCESSES TO PRODUCE HOMOGENIZED ALLOYS OF IMMISCIBLE METALS, PHASE 3 (TRW Systems Group) 53 p HC $4.50 CSCL 11F G3/26

N76-31329

Unclas
02427

EXPERIMENTAL DEVELOPMENT OF PROCESSES TO PRODUCE HOMOGENIZED ALLOYS OF IMMISCIBLE METALS: PHASE III

By J. L. Reger
TRW Systems Group
Redondo Beach, California

August 1976

Prepared for

NASA - GEORGE C. MARSHALL SPACE FLIGHT CENTER
Marshall Space Flight Center, Alabama 35812

TECHNICAL REPORT STANDARD TITLE PAGE

1 REPORT NO.	2. GOVERNMENT ACCESSION NO.	3. RECIPIENT'S CATALOG NO.
NASA CR-149977		

4 TITLE AND SUBTITLE	5. REPORT DATE
Experimental Development of Processes to Produce Homogenized Alloys of Immiscible Metals, Phase III	August 1976
	6. PERFORMING ORGANIZATION CODE
7. AUTHOR(S) J. L. Reger	8. PERFORMING ORGANIZATION REPORT #
9 PERFORMING ORGANIZATION NAME AND ADDRESS	10. WORK UNIT NO.
TRW Systems Group Redondo Beach, California	11. CONTRACT OR GRANT NO. NAS8-27805
	13. TYPE OF REPORT & PERIOD COVERED
12 SPONSORING AGENCY NAME AND ADDRESS	Contractor
National Aeronautics and Space Administration Washington, D. C. 20546	14. SPONSORING AGENCY CODE

15 SUPPLEMENTARY NOTES

16. ABSTRACT

An experimental drop tower package was designed and built for use in the MSFC 4-second drop tower. This effort consisted of a thermal analysis, container/heater fabrication, and assembly of an expulsion device for rapid quenching of heated specimens during low-gravity conditions. Six gallium-bismuth specimens with compositions in the immiscibility region (50 a/o of each element) were processed in the experimental package: four during low-gravity conditions and two under a one-gravity environment. One of the one-gravity processed specimens did not have telemetry data and was subsequently deleted for analysis since the processing conditions were not known. Metallurgical, Hall effect, resistivity, and superconductivity examinations were performed on the five specimens. Examination of the specimens showed that the gallium was dispersed in the bismuth. The low-gravity processed specimens showed a relatively uniform distribution of gallium, with particle sizes of 1 μm or less, in contrast to the one-gravity control specimen. Comparison of the cooling rates of the dropped specimens versus microstructure indicated that low cooling rates are more desirable. The Hall effect and resistivity measurements demonstrated that all of the specimens exhibited characteristics different from either pure bismuth or gallium, indicating the samples were behaving similarly to heavily doped extrinsic semiconductors. The superconductivity tests gave very anomalous results between the one-gravity and the low-gravity specimens, suggesting that large internal pressures and/or bulk surface effects between the two elements were making the processed specimens behave more like gallium deposited films, γ Ga or Bi III at high pressures.

17 KEY WORDS	18 DISTRIBUTION STATEMENT
	Unclassified — Unlimited /Kay V. Hainbuch, for Charles A. Lundquist Director, Space Sciences Laboratory

19 SECURITY CLASSIF. (of this report)	20. SECURITY CLASSIF. (of this page)	21. NO. OF PAGES	22 PRICE
Unclassified	Unclassified	52	NTIS

FOREWORD

This report was prepared by TRW Systems Group, Redondo Beach, California, and contains the results of the Phase III work accomplished during the period 7 December 1971 to 15 December 1972. The results from the Phase I task are documented in TRW Systems Report No. 18677-6006-RO-00, September 1971, and the results from the Task II efforts are documented in TRW Systems Report No. 18677-6008-RO-00, November 1971. The program was originated and is managed by the George C. Marshall Space Flight Center under the technical direction of Mr. I. C. Yates, Jr.

The work performed on the program was accomplished by the Advanced Technology Division of TRW Systems Group. Technical direction of the program is provided by the Materials Science Staff of the Research and Technology Operations. The Program Manager is Mr. R. L. Hammel and the Principal Investigator is J. L. Reger. Responsible technical personnel who supported this program are acknowledged below:

Dr. W. T. Anderson, Materials Science Staff

Mr. R. A. Mendelson, Materials Science Staff

Mr. V. H. Reineking, Materials Science Staff

Mr. C. Salts, Jr., Materials Science Staff

Mr. R. Valencia, Jr., Materials Science Staff

Acknowledgement is gratefully extended to Professor A. Yue of U.C.L.A. for his assistance in performing the Hall measurements.

TABLE OF CONTENTS

FIGURES

FIGURES

(CONTINUED)

TABLES

1.0 INTRODUCTION

The opportunities for utilizing manned space flights to obtain near weightless conditions for processing immiscible systems into homogenized or metastable metal alloys or other materials will be severely limited until the space shuttle is operational. Since much preliminary information and experimentation is required in order to assess the potential usefulness and process requirements of immiscible systems, it was decided to assess the capabilities of the MSFC drop tower as a short duration, low gravity facility for processing immiscible metal systems. The system gallium-bismuth, in equal atomic percentages, was chosen as the binary pair for processing and study. This required a thermal analysis of the complete system, fabrication of the container/heater experiment package, assembly of the expulsion device, establishment of the operational mode of the drop package and examination of the processed specimens, both metallurgically and for their electronic properties.

Each of these areas is discussed separately, with the conclusions delineated at the end of the report.

2.0 THERMAL ANALYSIS

From the standpoint of an assumed 3.5 second nominal free fall time in the MSFC drop tower, it was decided to utilize the gallium-bismuth couple for the initial thermal analysis and tests. This consideration was based on the following: (1) the consulate or complete miscibility temperature is approximately 250°C at 50 a/o gallium (Figure 1), (2) there is a possibility that the couple, if sufficiently homogenized, may be a potential extrinsic semiconductor [Reference 1], and (3) the materials are easily handled in this temperature regime and pose no particular safety hazard except from the thermal aspect during initial processing.

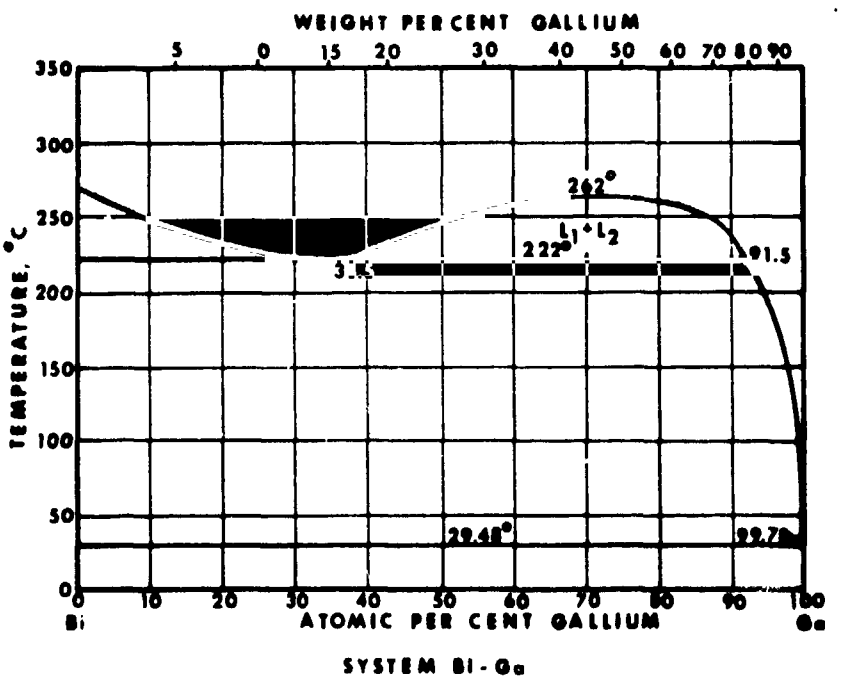

Figure 1. Phase Diagram of the Bismuth-Gallium Binary Couple

The sample size was optimized with respect to required final temperature after drop, maximum achievable heat transfer, and design considerations for the container and heater configuration. The final temperature at the end of the free fall must be less than 29°C, the

melting point of gallium (and preferably much lower). Maximum achievable heat transfer is accomplished by flat plate geometries, with turbulent flow of the cooling fluid. In order to minimize thermal backflow from the heater and container support, the heat flux was assumed to be primarily by radiation and still air convection through an annular space between the container and the heater element. Previous thermal calculations on the heating rate of a gallium-bismuth couple of larger dimensions [Reference 2] showed that acceptable heating times could be achieved for power inputs between 15 and 34 watts. Final power input for heating (to be discussed later) was 22 watts. This corresponds to a watt density input of 3 watts per cm^2 (20 W/in^2) for the capsule, which is one-half the recommended still air watt density value for the heater element used.

The internal container dimensions utilized for calculating the drop tower experiment cooling curves are 1.27 cm (0.5 in.) long by 0.635 cm (0.25 in.) wide by 0.318 cm (0.125 in.) thick. The container material is tantalum with a wall thickness of 0.025 cm (0.010 in.). However, since bismuth has a lower thermal conductivity than either tantalum or gallium, the container wall was assumed to be bismuth to obtain the cooling curves. In all cases, the calculations assume worst case conditions where necessary in order to assure that the drop time limitations could be met. Figure 2 illustrates the container cooling times at the centerline of the specimen for three heat transfer coefficients. An initial coolant water temperature of approximately 0°C was assumed since the pre-drop time after the loading of the water should be minimal. As can be seen, the heat transfer coefficient must be higher than 0.568 watt/cm^2 °C (1000 BTU/hr ft^2 °F) in order to cool the specimen in 3.5 seconds or less. Additional calculations were made to determine the waterflow necessary to achieve the higher heat transfer values. For a flow velocity of 6.1 m/sec (20 ft/sec) through a constricted annulus of 0.32 cm (0.125 in.), the flow rate is 0.84 kg/sec (1.85 lb/sec) for a pressure drop of approximately 3.5 kN/m^2 (0.5 psi). This corresponds to a heat transfer coefficient of 5.08 watt/cm^2 °C (8950 BTU/hr ft^2 °F) if

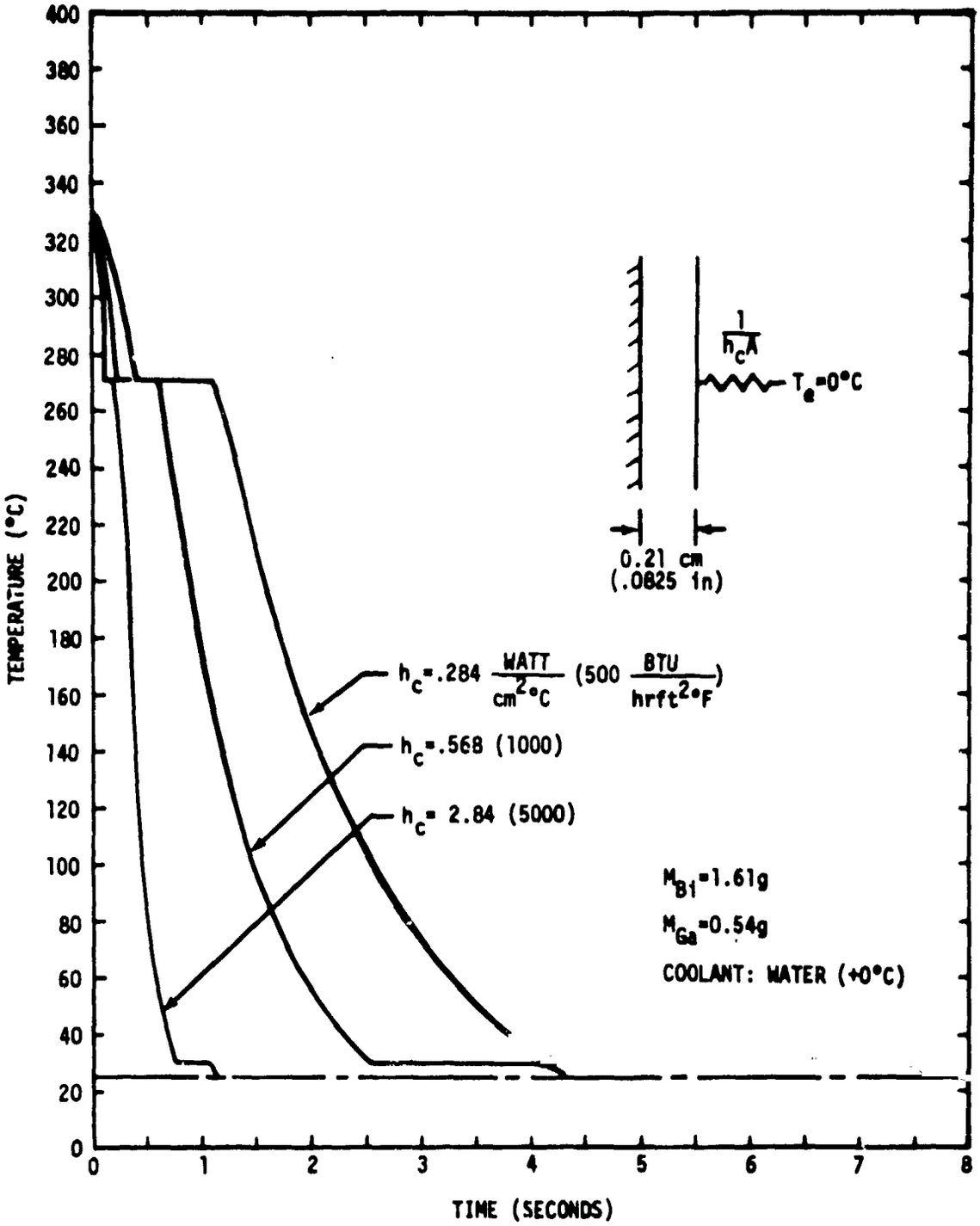

Figure 2. Drop Tower Cooling Times as a Function of Heat Transfer Coefficients.

the flow is turbulent, or 2.84 watt/cm^2 °C (5000 BTU/hr ft^2 °F) for laminar flow. Since the Reynolds number is approximately 100,000, which is in the transition region, the lower coefficient value was used for calculating the maximum cooling curve shown in Figure 2. Since both conservative designs and thermal calculations were utilized, the desired cooling rate was considered to correspond to a heat transfer coefficient value between 0.568 and 2.84 watt/cm °C. Thus the flow rate goal of the expulsion device was aimed at achieving a discharge rate of 0.84 kg/sec.

3.0 CONTAINER/HEATER FABRICATION

3.1 Container Fabrication

As mentioned previously, the container was constructed of commercially pure tantalum sheet 0.025 cm (0.010 in.) thick. Fabrication consisted of the following steps.

The sheet was formed over a machined rectangular ba of OFHC copper to obtain a hollow rectangular tube 18 cm (7 in.) long. An unwelded, formed but rejected tantalum tube and the copper forming bar are shown in Figure 3. The tantalum tube with the copper bar still inserted was then electron beam (E-B) welded down one edge to form a welded seam. Previous attempts to conventionally weld the tantalum were unsuccessful, so all welding steps utilized E-B welding.

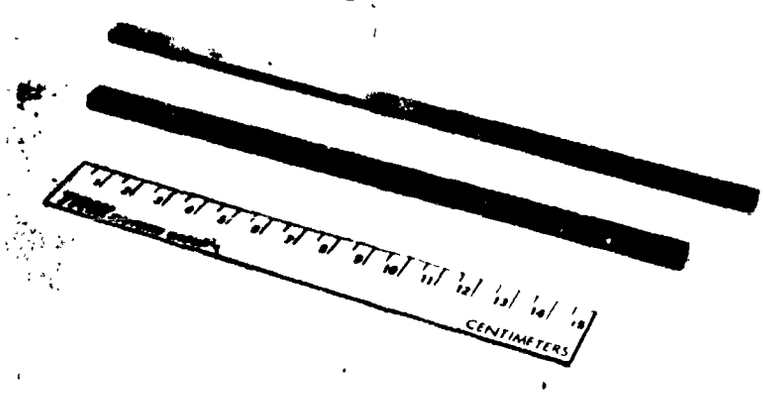

Figure 3. Copper Forming Bar and Unwelded Tantalum Tube

The welded tube was then cut into sections 1.31 cm (0.165 in.) long, and both ends tabbed 0.051 cm (0.020 in.) on all four sides. A tabbed container with unattached end caps is illustrated in Figure 4.

All of the parts (tabbed containers and end caps) were then cleaned in hot concentrated nitric acid, rinsed in distilled water and dried. The bottom end cap was spot welded to the tabbed container for E-B welding adjustment, a copper heat sink inserted into the container, and the bottom end cap E-B welded to the container. Figure 5 illustrates a container with one end welded and the heat sink in place. Each welded container was leak checked by the air bubble test.

Nine containers were acceptable, and were loaded with gallium and bismuth. The bismuth was obtained from Alfa Inorganics as M6N5 pure metal chips (metallic purity: 99.99995%). The gallium was obtained from Alcoa as M5N+ pure metal. Each metal was weighed to give a 50 a/o composition for each container. The metals were separately loaded (bismuth first) by vacuum induction melting the metal into the container and cooling under research grade argon. Very little oxidation, if any, was evident after processing each metal. A small (approximately 0.2 cm^3) expansion volume was left in each capsule. Although both gallium and bismuth expand upon solidification, the expansion at the higher processing temperatures and final E-B welding precluded total filling of the container.

After the metals were loaded into the containers, the top end caps were spot welded to the containers and E-B welded shut. Complete closure was established by filing away part of the weld and microscopic examination to determine that the weld penetration was continuous and complete. Figure 6 is a photomacrograph of a filled, completed container.

3.2 Heater Fabrication

The heater container has a number of functions it must perform: (1) it must be able to heat the gallium-bismuth to the processing

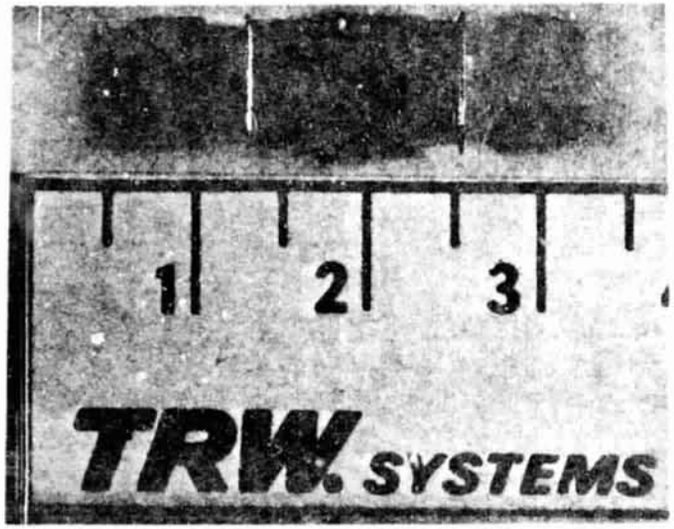

Figure 4. Tabbed Tantalum Container With End Caps (Original Magnification; 3X)

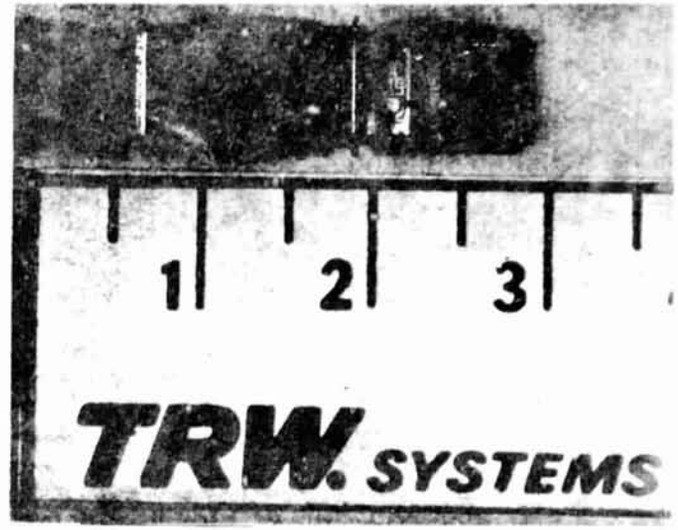

Figure 5. Tantalum Container; One End Welded With Inserted Copper Heat Sink and Top End Cap (Original Magnification; 3X)

Figure 6. Filled Tantalum Sample Container (Original Magnification; 3X)

temperature, (2) it must direct the cooling water annularly around the sample container, (3) it must keep the sample container in position during the test, and (4) it must not reradiate any significant thermal energy back to the sample container after the end of the test.

Inconel sheathed Nichrome heating elements were utilized (XacTglo element no. 601-1103-001) since they can be shaped, brazed and handled without danger of shorting during assembly. The elements were wound around a 0.95 cm (0.375 in.) by 1.90 cm (0.75 in.) mandrel, removed, and the wound element separated to a total length of 0.27 cm (0.50 in.). The formed heater element was then brazed to the bottom plate of a series 304 stainless steel enclosure with 0.48 cm (0.187 in.) Transite insulation between the heater element and the stainless wall. The two sides of the enclosure were then spot welded to the bottom plate, again with Transite insulation between the stainless sides and the heater element. The sample container was then clamped in place with 0.025 cm (0.010 in.) stainless steel support brackets, spot welded, and the top plate then similarly spot welded in place. Finally, the brazed AN fitting with the water inlet tubing was attached. Figure 7 shows a somewhat exploded view of the various elements making up the complete heater/container assembly, and Figure 8 shows a fabricated heater assembly from the water outlet end. This particular assembly was used to demonstrate feasibility of the complete experiment package as discussed in Section 4. Figure 9 is a cross-sectional view perpendicular to the flow path schematically illustrating the various positions of the major components of the heater/sample container assembly.

After the heater assembly was complete, nickel wire was silver brazed to the Nichrome heating wire and the exposed heating element insulation protected with a coating of Sauereisen ceramic cement. Each heater assembly was checked for element resistance and any shorts. All assemblies were satisfactory, with an element resistance of 35 ohms.

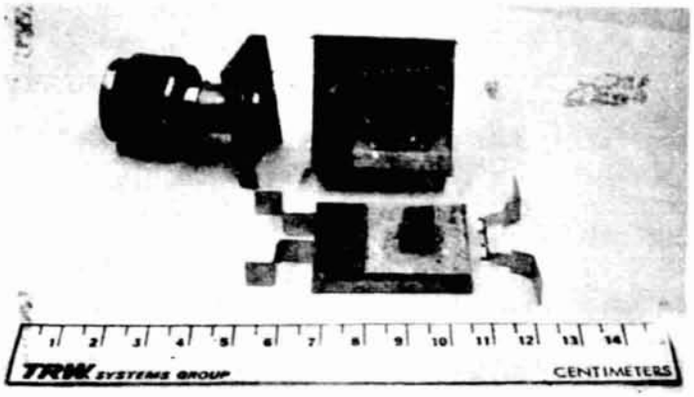

Figure 7. Exploded View of the Heater/Container Assembly

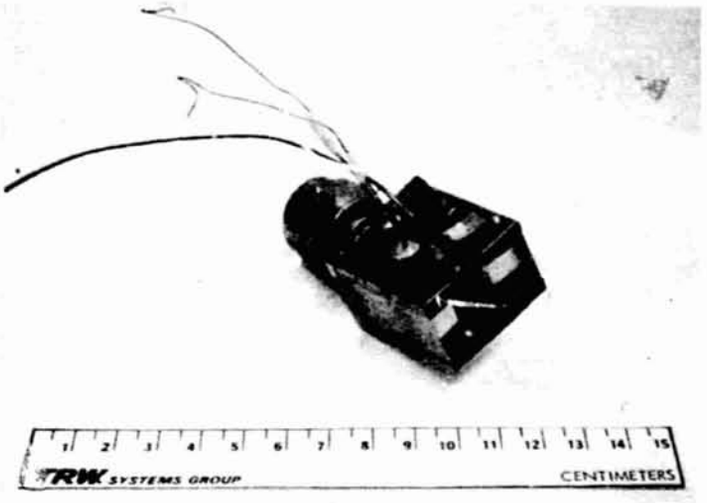

Figure 8. End View of Completed Heater/Container Assembly

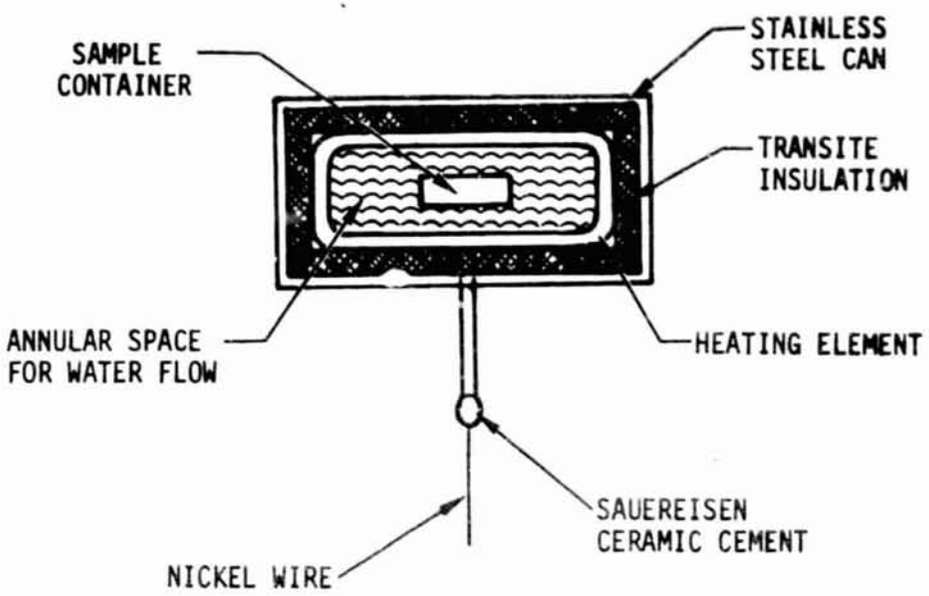

Figure 9. Cross-Section of Heater/Container Assembly

4.0 EXPULSION DEVICE ASSEMBLY

4.1 Major Part Description

Figures 10 through 13 show the expulsion device assembly at approximately 90° rotation angles, and Figure 14 is a close-up photograph of the fitting and terminal strip where the experiment is to be connected. Each major sub-element is labled and described below.

4.1.1 E-1: Expulsion Tank

The expulsion tank is a surplus Surveyor liquid propulsion tank (S/N 159) with a Teflon bladder. There is an interior vent line for filling which extends vertically from the bottom of the tank. The exterior shell is stainless steel, and the original working pressure was 4000 kN/m^2 (600 psig). The tank has been proofed to 3100 kN/m^2 (450 psig) and the recommended working pressure is 2400 kN/m^2 (350 psig).

Figure 10.

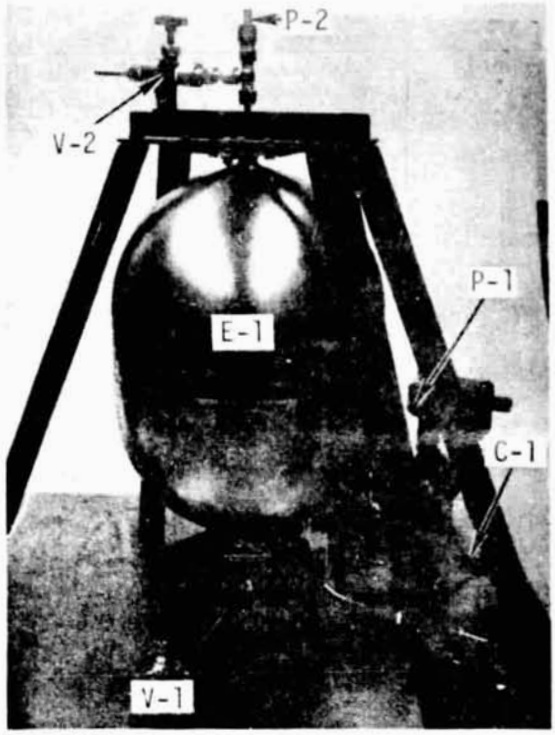

Figure 11.

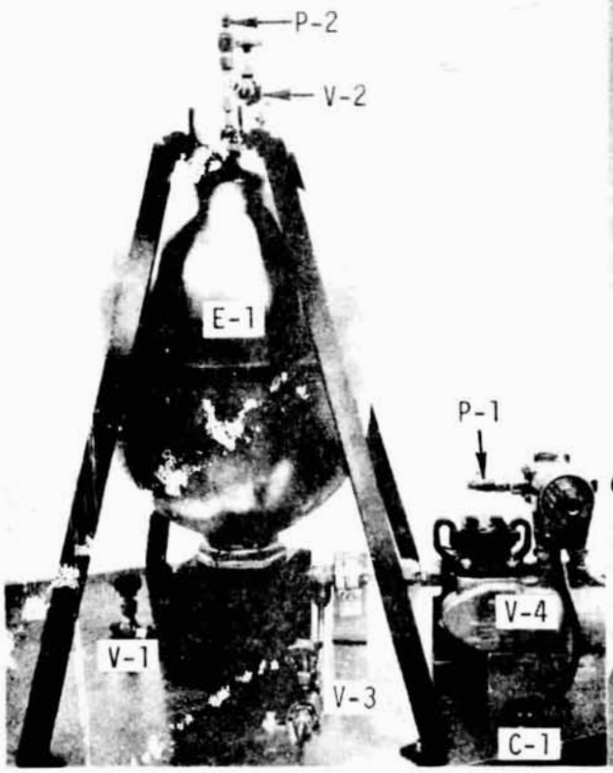

Figure 12.

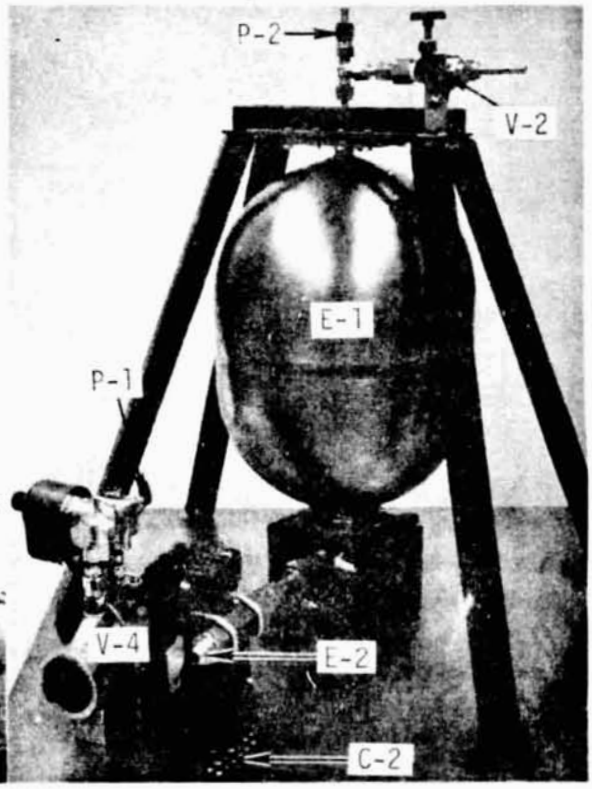

Figure 13.

EXPULSION DEVICE ASSEMBLY WITH MAJOR FUNCTIONAL ELEMENTS MARKED

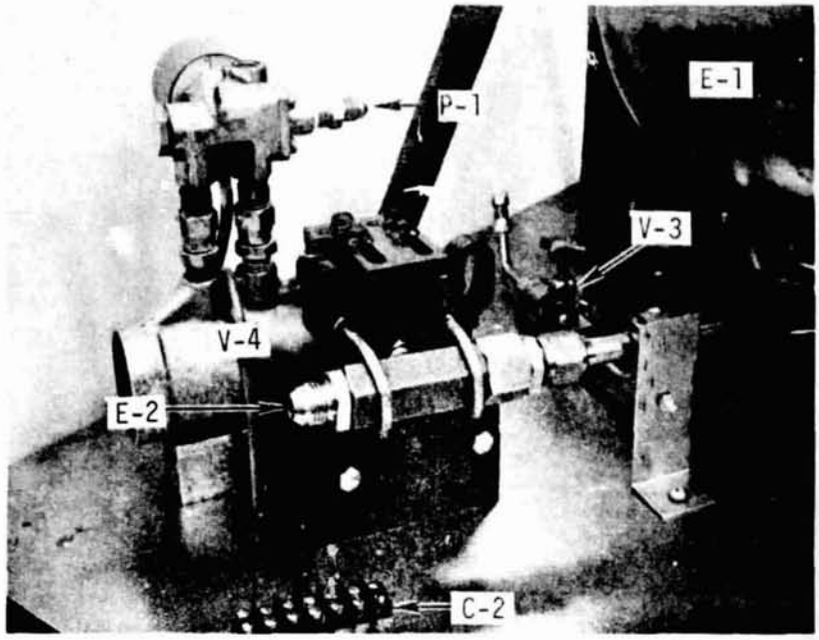

Figure 14. Close-up Photograph of Experiment Container Connection Area

4.1.2 E-2: Experiment Attachment Fixture

This fixture is a AN 1.27 cm (0.5 in.) fitting attached to the master remote control valve (V-4). The experiment container has the corresponding female fixture brazed to the entrance and is easily connected. The heater and thermocouple leads are connected to the terminal strip C-2.

4.1.3 V-1: Bladder Vent Valve

This valve is connected to the inner vent line and serves both as the air leak-in when expanding the bladder before filling and the air leak-out when filling the tank with the coolant.

4.1.4 V-2: Vacuum/Vent Valve

This valve is connected to the outer metal shell and serves two purposes: (1) a slight vacuum is pulled through V-2, with V-1 open, to expand the bladder to the outer wall, and (2) the gas pressure is vented through it when the test is over to relieve the expulsion pressure on the bladder.

4.1.5 V-3: Liquid Fill Valve

This valve is used to fill the tank with the cooling water, and to empty the tank after the tests are complete.

4.1.6 V-4: Master Remote Control Valve

This valve connects to the experiment and is the valve that will be remotely operated during the test.

4.1.7 C-1: Solenoid Connection for Gas Actuated Pilot Valve

This terminal strip serves as the connection point for the 28-30V remote controlled power supply. The solenoid actuates the pilot valve which opens the master remote control valve during test. When the voltage is removed, the master remote control valve automatically closes.

4.1.8 C-2: Experiment Terminal Strip

This terminal strip connects the external 28-30V power source and the thermocouple leads to the experiment.

4.1.9 P-1: Gas Actuated Pilot Valve Connection

This valve connection operates the pilot valve through actuation of the solenoid. The valve actuates through a pressure range of 69 to 970 kN/m^2 (10-140 psig). Since the actuation time of the master remote control valve is dependent upon the pressure actuating the pilot valve, it is recommended that a pressure of 689 kN/m^2 (100 psig) be used.

4.1.10 P-2: Main Pressurization Line

This line connects to the main pressurization tank and the gas accumulator tank for expulsion of the cooling water through the experiment during the drop. As mentioned previously, the recommended working pressure is 2400 kN/m^2 (350 psig). Further, since it is undesirable to suddenly pressurize the tank, it is recommended that the pressure be

applied reasonably slowly to the working pressure (approximately 970 kN/m^2 or 140 psig per minute).

4.2 Expulsion Device Fabrication

The primary problem in assembling the expulsion device was to obtain the correct flow rate within the desired expulsion pressure level. The primary outlet from the expulsion tank is a 0.952 cm (0.375 in.) line, which is fixed. The gas pressure expulsion line is also fixed at 0.635 cm (0.25 in.). The vent line is 0.317 cm (0.125 in.) but this is immaterial since it is closed during actual test, and does not interfere with the pre-test loading operation.

Preliminary tests with the original outlet line showed that it was not possible to obtain a flow rate anywhere close to 0.84 kg/sec at pressures up to 2400 kN/m^2.

Two major alternations were required: (1) transition of the outlet line to a larger diameter to reduce pressure drop to the experiment outlet, and (2) addition of a gas accumulator to maintain constant expulsion pressure during the run.

The final outlet line was sized at 1.27 cm (0.500 in.) along with an open oriface ball valve at the master remote control valve (V-4). In order to reduce pressure losses at the transition point, the 0.952 cm outlet line was gradually flared to the 1.27 diameter over a 1.9 cm length and brazed to a AN tee. The fill line (V-3) was brazed to the branch and a minimal length of tubing connected to the control valve (V-4).

An 8.6 liter (2.3 gallon) high pressure accumulator was added to the gas pressurization line via a tee fitting between the main gas regulator and the expulsion tank (E-1). All plumbing was done with 0.635 cm (0.25 in.) tubing, although some advantage might have accrued by using 0.952 cm (0.375 in.) diameter tubing to the tank (E-1), again making a 2X diameter transition flaring from the smaller tubing to the larger.

All components were structurally braced and anchored to a 0.61 M (2 ft.) square, 1.27 cm (0.50 in.) thick aluminum plate. This plate was assembled in the main drop tower assembly box.

A number of runs using ambient water were made on the assembled apparatus for various flow times. In all cases, runs exceeding two seconds gave the desired flow rate (measured volumetrically as a function of flow time) of 0.84 kg/sec or greater. Runs less than 2 seconds gave slightly less flow rate, but this is probably due to the delay time for full opening of the master remote control valve (V-4). This delay time was estimated to be 0.2 seconds.

5.0 MODE OF OPERATION

Figure 15 schematically illustrates the experimental set-up at TRW for functional testing the complete apparatus. The following operational sequences were followed.

1. Attach the experiment container to fixture E-2. Attach heater and thermocouple leads to connector C-2, and connect corresponding leads to MSFC control panel. Energize heater and monitor temperatures. (Heater voltage can be 28-30 volts. Thermocouple is Chromel-Alumel).

2. Attach pilot valve gas pressure supply to pilot valve P-1.

3. Attach expulsion gas pressure supply line to line P-2.

4. Attach solenoid connection lines from control panel to C-1. (The voltage may be 28-30 volts).

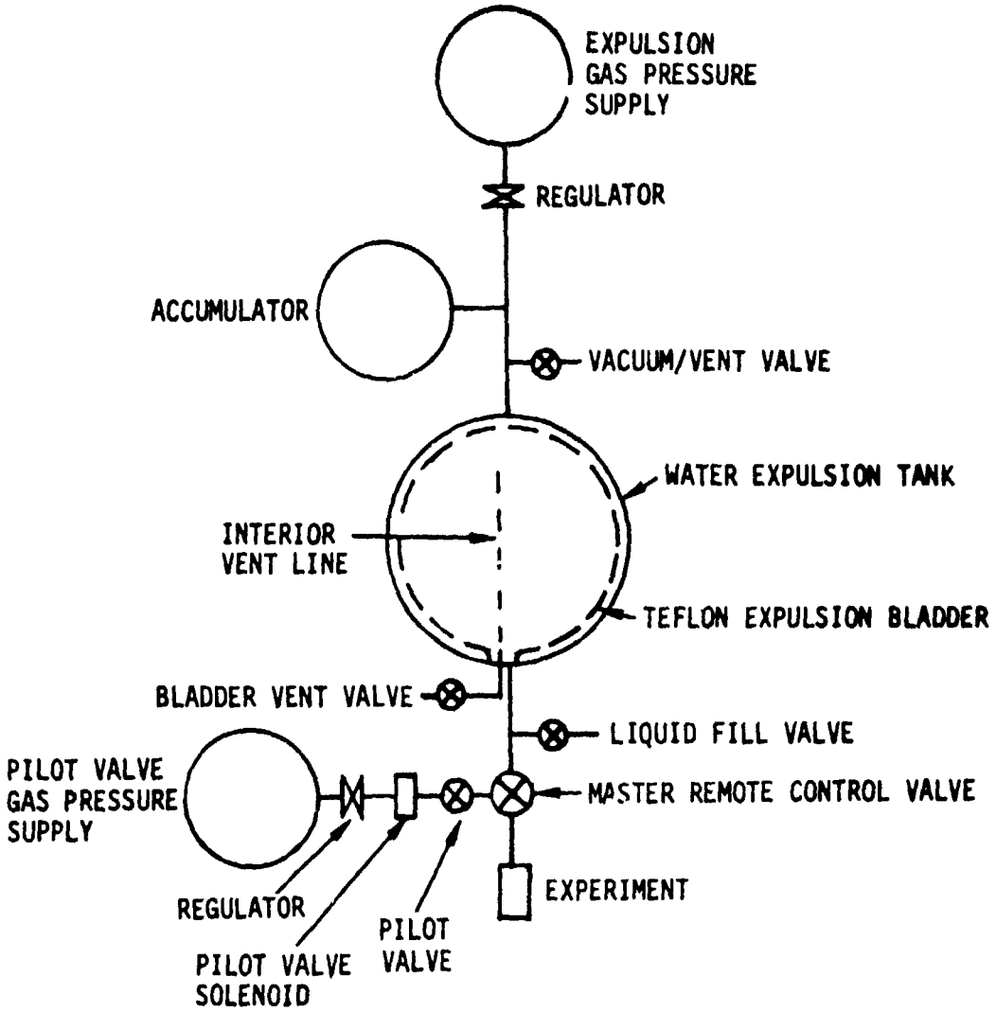

Figure 15. Schematic of Experimental Apparatus

5. Open bladder vent valve V-1.

6. Attach a vacuum line to the vacuum/vent valve V-2. A small fore pump vacuum system is sufficient.

7. Pull a vacuum until valve V-1 no longer pulls a suction.

8. Close valve V-2.

9. Open fill valve V-3 and attach a rubber hose to the line. Use an immersion or centrifugal pump to pump the chilled (0-2°C) water into expulsion bladder E-1. (This time may take 5-10 minutes, depending on pump). Fill with 7 liters (∿4 gallons) of water.

10. Close valves V-1 and V-3.

11. Pressurize pilot valve solenoid line P-1.

12. Pressurize expulsion tank E-1 to 2400 kN/m^2 (350 psig). (This should be done at a rate of 689 kN/m^2 (100 psig) per minute.)

13. Observe thermal history of experimental apparatus. The heating time is about 30 minutes to reach approximately 330°C (620°F) and the hold time for miscibility of the metals is another 15 minutes.

14. After heating time, shut-off power, drop apparatus, and actuate pilot valve solenoid P-1.

15. Allow cooling water to flow for 6.5 seconds (3.5 seconds during drop and 3 seconds more to isothermalize heater, container, etc.). Automatically de-energize solenoid at C-1 after 6.5 seconds.

16. Remove experimental container and attach a new one.

17. Open vacuum/vent valve V-2 to depressurize system.

18. Repeat steps 1 through 17 as required.

Figure 16 shows a run utilizing the standard capsule/heating container. The water flow (temperature was 1-2°C during filling) was stopped after 3.5 seconds to determine the re-radiation after a simulated drop. The second 2 second flow should have been 3 seconds, but after 10 minutes, the apparatus had only re-thermalized to 25°C (77°F). Thus the flow after the apparatus has been dropped and is in the catch tube is merely to keep the experimental container cold. Since a minimal water supply should be in the tank during deceleration, the tank is not completely filled at start. However, to prevent damage to the bladder, a small amount of water is left after the drop.

The two runs at TRW demonstrated that the run procedure produces the cooling times required to lower the temperature of the sample to an acceptable value during the 3.5 second estimated drop time in the MSFC drop tower. Figures 17 and 18 are photographs of assembled drop package as integrated at MSFC. The expulsion device, experiment assembly and the electronic package are located in the top position of the housing and the pressurization bottles and waste water catch tank are mounted in the bottom position of the housing.

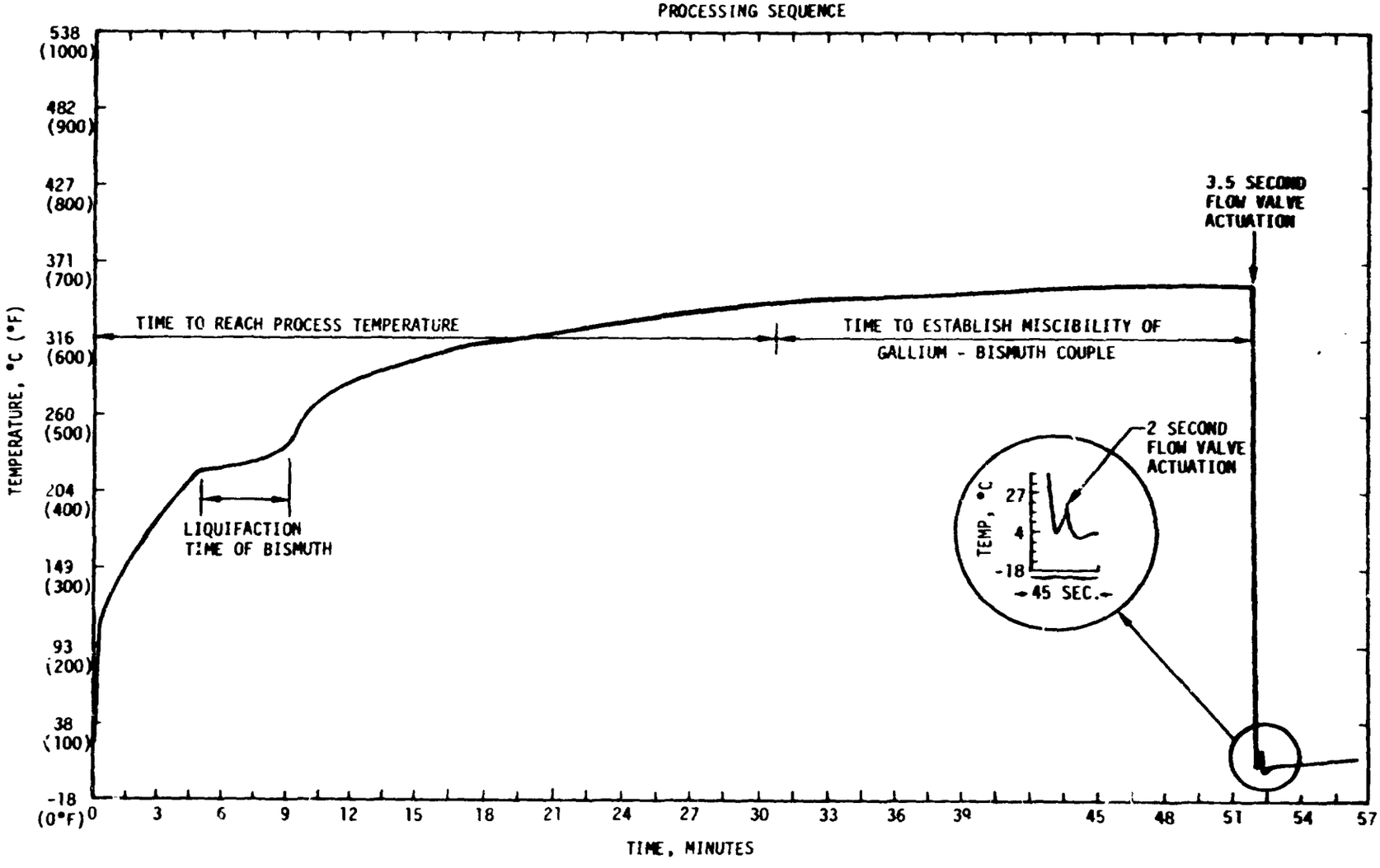

Figure 16. One Gravity Experiment Run

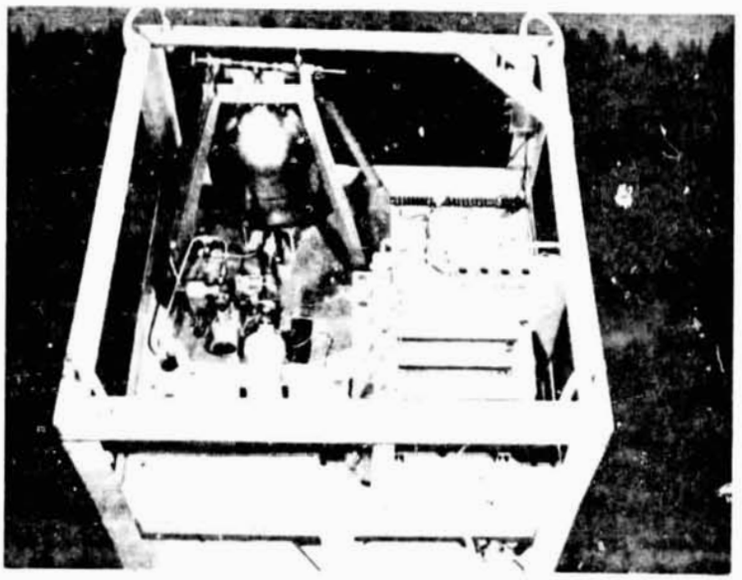

Figure 17. Assembled Drop Tower Package Showing Expulsion Apparatus

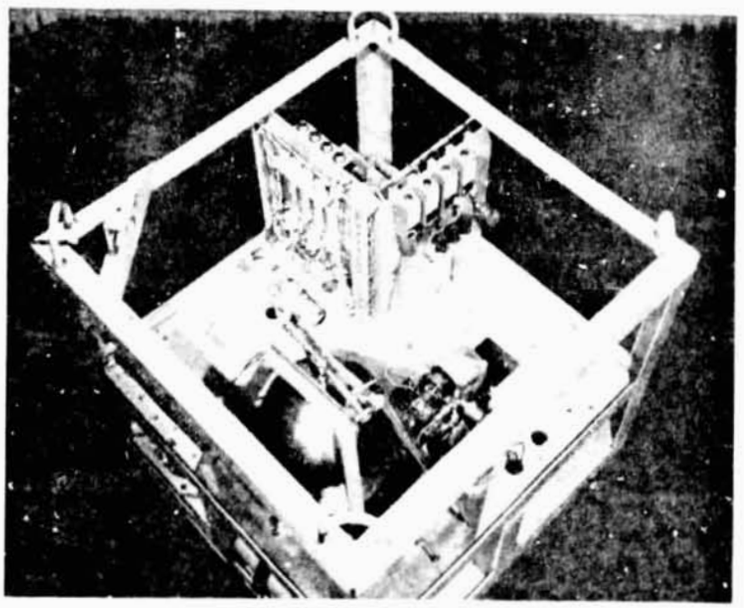

Figure 18. Assembled Drop Tower Packaging Showing Electronic Sequences and Telemetry Assembly.

6.0 METALLURGICAL EXAMINATION

6.1 Specimen Preparation

The gallium-bismuth specimens, as received from NASA/MSFC, were removed from the individual heater containers and marked with respect to their spatial position in the experiment (e.g., top end and which edge was closest to the main valve). This was felt necessary since, with the exception of the control specimen, the telemetered data of the drop specimens listed in Table 1 showed some process differences. The only telemetered data obtained for the control specimen was the initial and final temperatures. The tantalum containers were then removed and both the leading and trailing edge of the specimen were polished. Since gallium melts at 29.75°C (85.55°F), a special jig was fabricated to polish the specimens, and ice water was used as the coolant during polishing. The specimens were always handled with tweezers and kept refrigerated when not being examined or tested. A portable ice chest was used to transport the specimens when they were moved from building to building.

Examination of the two polished edges did not show any differences in appearance, even on the control (one gravity processed) specimen, therefore the requirements on the spatial control was eliminated.

6.2 Optical Examination

After the samples were polished, photomicrographs were taken of each specimen at 50, 100 and 1000X magnification. Typical areas are shown by the photomicrographs of Figures 19 and 19a. As can be seen in all cases, there is a significant difference between the control specimen (1-3) and the four specimens dropped from the drop tower. The gallium is dispersed in the bismuth, and except for the control, the majority of the gallium droplets are 1 μm or smaller in diameter. The gallium in the control sample does not appear to be interconnected, and has a rapidly quenched dendritic appearing microstructure. Since the criteria for establishing thermal convection cells is that the Rayleigh number

TABLE 1

TELEMETERED DATA FROM DROP TOWER EXPERIMENTS

SPECIMEN NO.	1-3 (CONTROL)	9-2	2-4	4-5	5-6
TEMPERATURE AT START OF DROP, °C	375	405	270	384	346
GRAVITY LEVEL AT START OF COOLING, g_e	1	-.038	-.038	(0)	(0)
GRAVITY LEVEL DURING COOLING, g_e	1	-.038	-.038	(0)	(0)
FINAL TEMPERATURE AT END OF DROP, °C (AT 4.3 SEC.)	25 (a)	2	2	2	11
INDICATED COOLING RATE, °C/SEC. (b)	N/A	7000	5800	6400	5200

(a) AFTER APPROXIMATELY 5 MINUTES.

(b) ACTUAL COOLING TIMES LESS THAN 100 MILLISECONDS.

Figure 19. Photomicrographs of Specimens

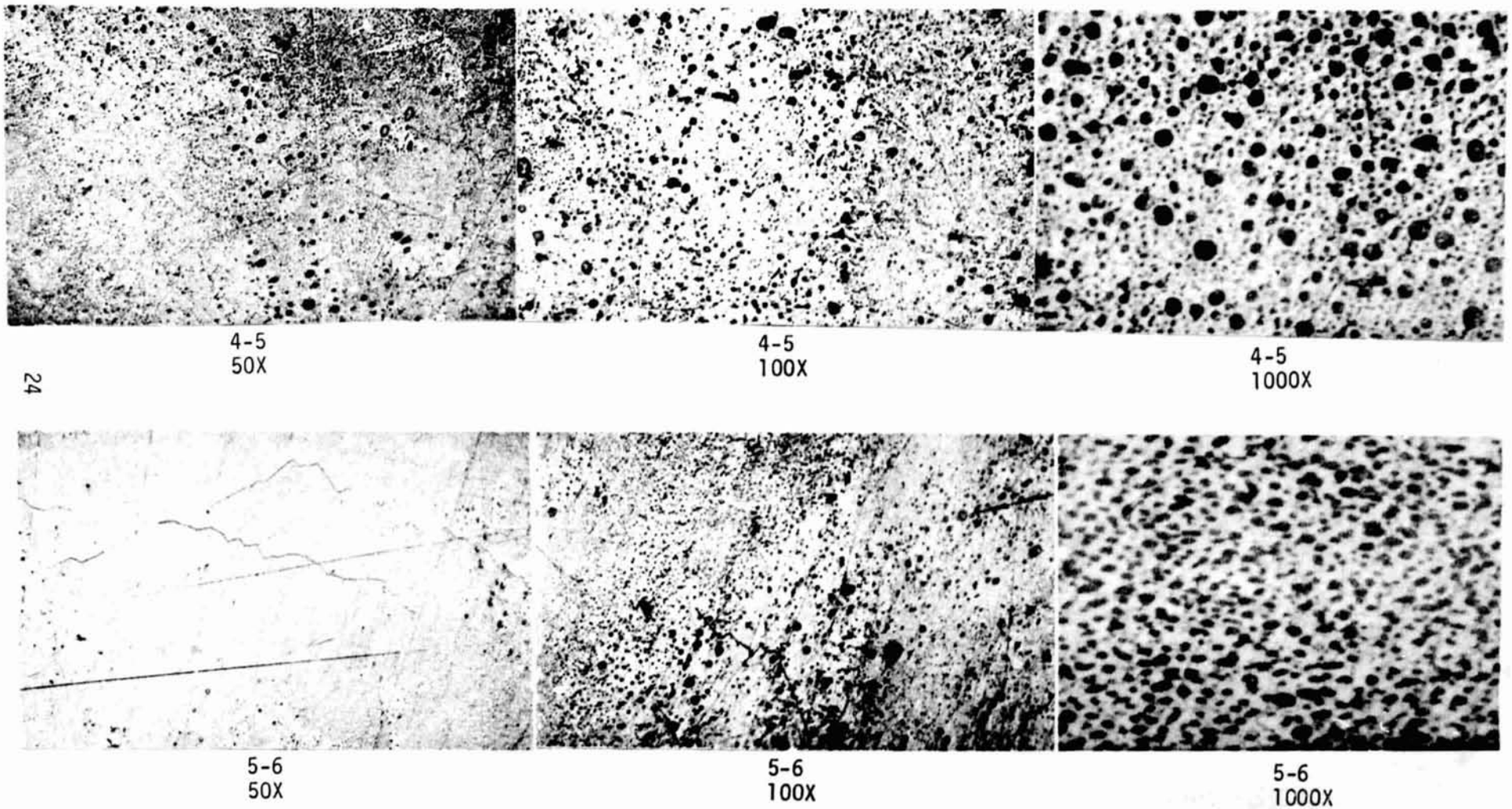

Figure 19a. Photomicrographs of Specimens

$Re = \frac{g\alpha\beta d^4}{k\nu} \geq 1700$ [Reference 3] where:

g = acceleration
β = temperature gradient
α = coefficient of thermal expansion
d = characteristic dimension
k = thermal diffusivity
ν = kinematic velocity

calculations were made using averaged physical values [Reference 21] of the gallium-bismuth mixture contained in the capsule, with the characteristic dimension being either the long or the transverse dimension of the capsule. These calculations were done using 980 cm/sec^2 for the control and 39.2 cm/sec^2 for the low gravity specimens and various differential temperatures. The minimum Rayleigh number for the control was approximately 5400, while the maximum Rayleigh number for the dropped specimens is approximately 170. There is a time lapse of approximately 0.25 to 0.5 seconds before the bismuth solidifies, as shown in Figure 2, which is sufficient for convection cells to form and give rise to the structure found for Specimen 1-3. The Froude number is less than unity for all specimens, thus unusual sedimentation effects should not be present [Reference 3], as shown in Figures 19 and 19a. The four dropped specimens appear to have "grain boundaries". The exact meaning of this aspect is not clear, although the boundaries appear to be composed primarily of gallium. Since both gallium and bismuth expand on solidification, it may be a pressure effect. This is discussed further in Section 7.2

6.3 Scanning Electron Microscopy

The specimens were examined with the scanning electron microscope (SEM) in order to determine in more detail the morphological features of the specimens. Figure 20 shows the specimens at 100, 1000 and 10,000X magnification. The white material is alumina that was used to polish the specimens and became imbedded in the gallium.

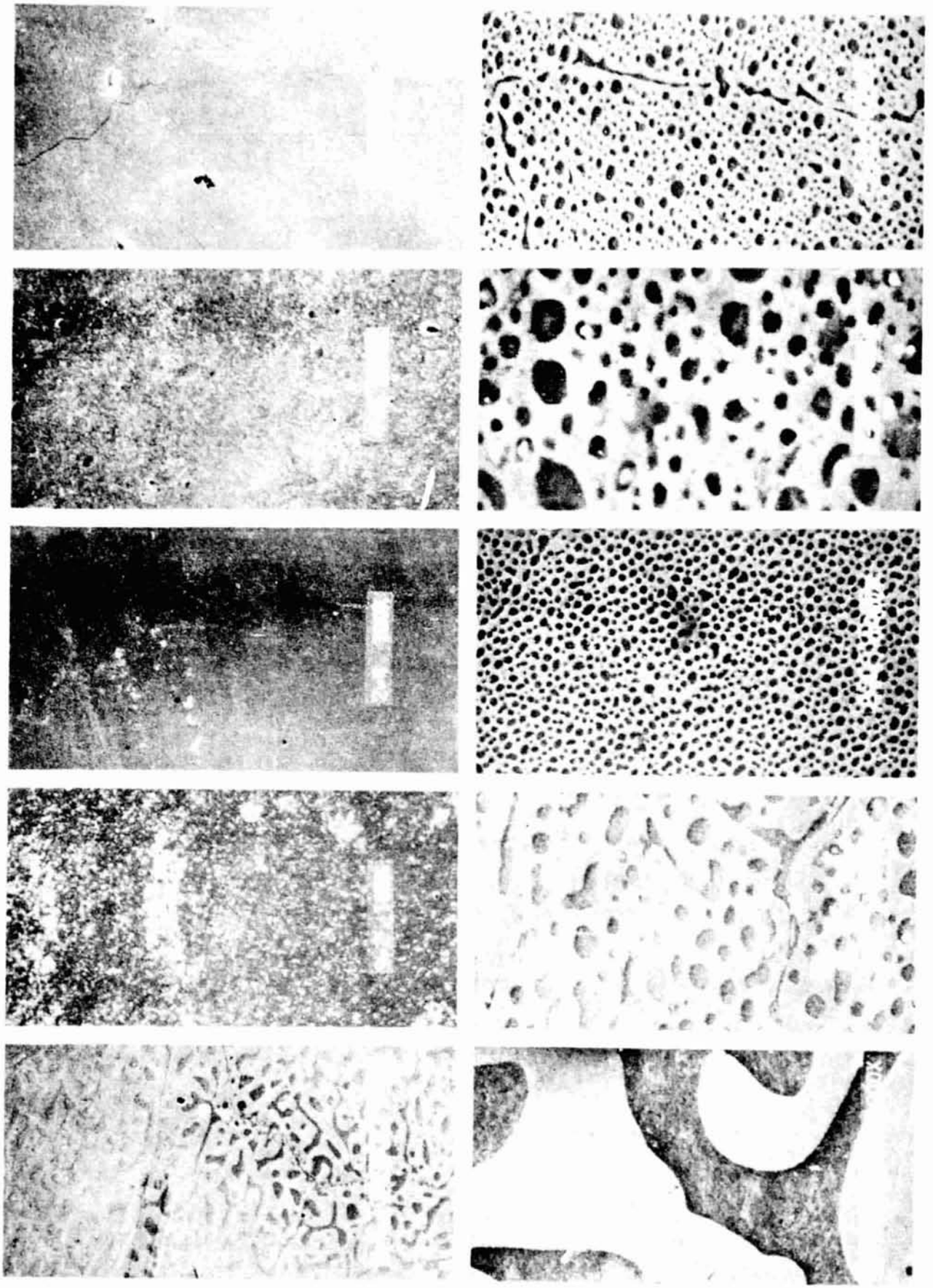

Figure 20. Scanning Electron Photomicrographs of Specimens.

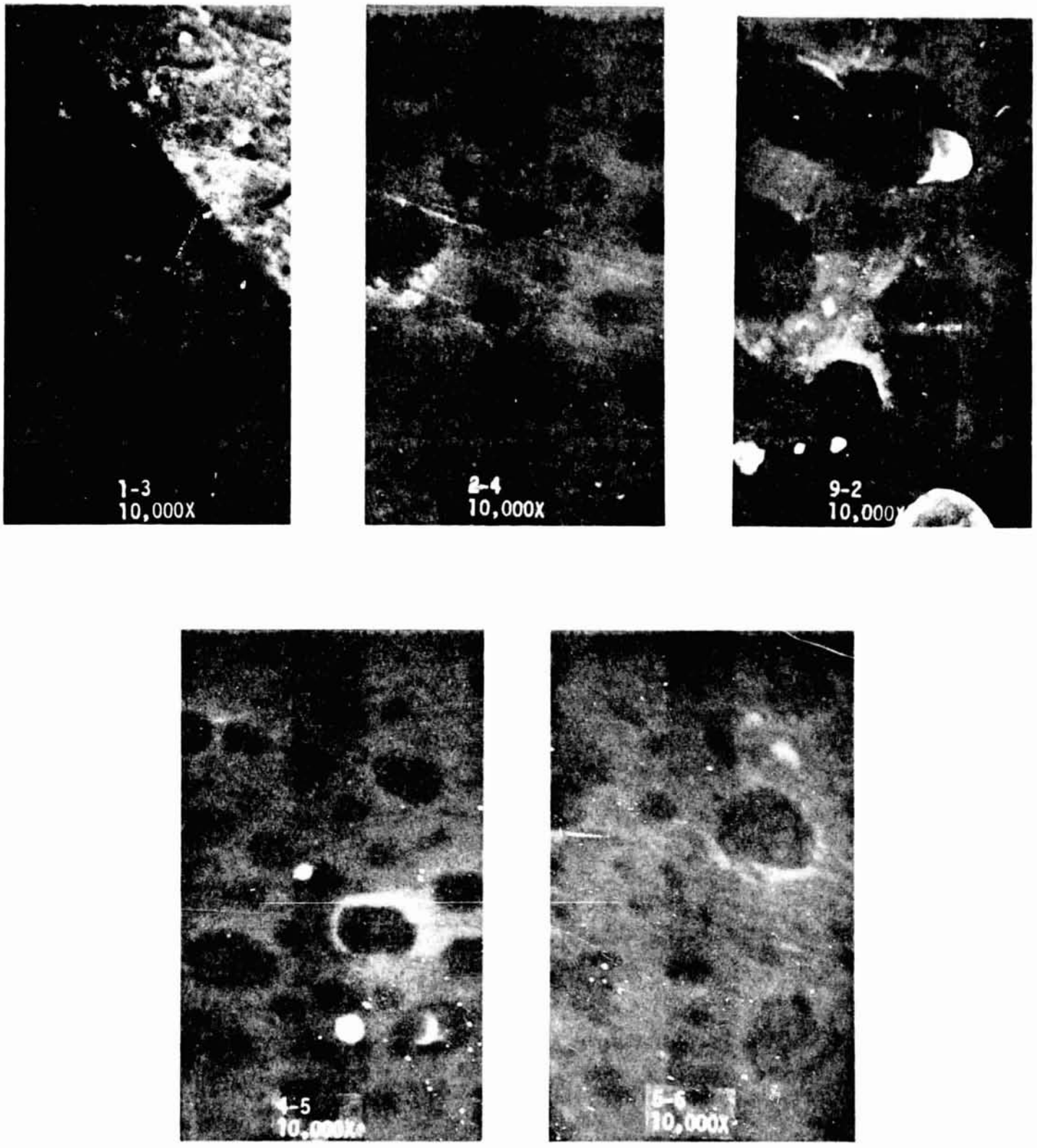

Figure 20a. Scanning Electron Photomicrographs of Specimens.

The most interesting features are (1) the "grain boundaries" are gallium, (2) the gallium droplets are somewhat distorted, indicating that the high cooling rates shown in Table 1 caused some surface tension interaction, and (3) the higher cooling rates for specimens 9-2 and 4-5 apparently affected the gallium droplet size.

6.4 Electron Microprobe Analysis

Attempts were made to analyze the specimens by microprobe analyses. Due to the 1 μm beam size, only the control specimen could be properly scanned. Figure 21 illustrates the scan obtained with the control specimen and dropped specimen 9-2. Even at a higher magnification, 9-2 could not be resolved. It was possible, however to verify that gallium was the dispersed phase. Line scanning indicated little or no alloying between the gallium and bismuth, in accord with the phase diagram.

7.0 ELECTRONIC PROPERTIES

7.1 Hall Effect and Electrical Resistivity Measurements

Longitudinal samples approximately 1 mm thick were sliced from each specimen with a wire saw, using an ice water-silicon carbide slurry as the cutting compound. Hall effect voltages were measured at U.C.L.A. in their equipment and the bulk resistivities at TRW on a Leeds four-point guarded probe at room (∿23°C) and dry ice (-78°C) temperatures.

Table 2 lists the Hall coefficient, the two resistivities, and the Hall mobility values. The following deductions may be made:

1. The Hall coefficient is of the same order as polycrystalline bismuth although somewhat smaller and has a similar magnetic field dependence. In the single energy band model (electron carriers only) the decrease in the Hall coefficient represents

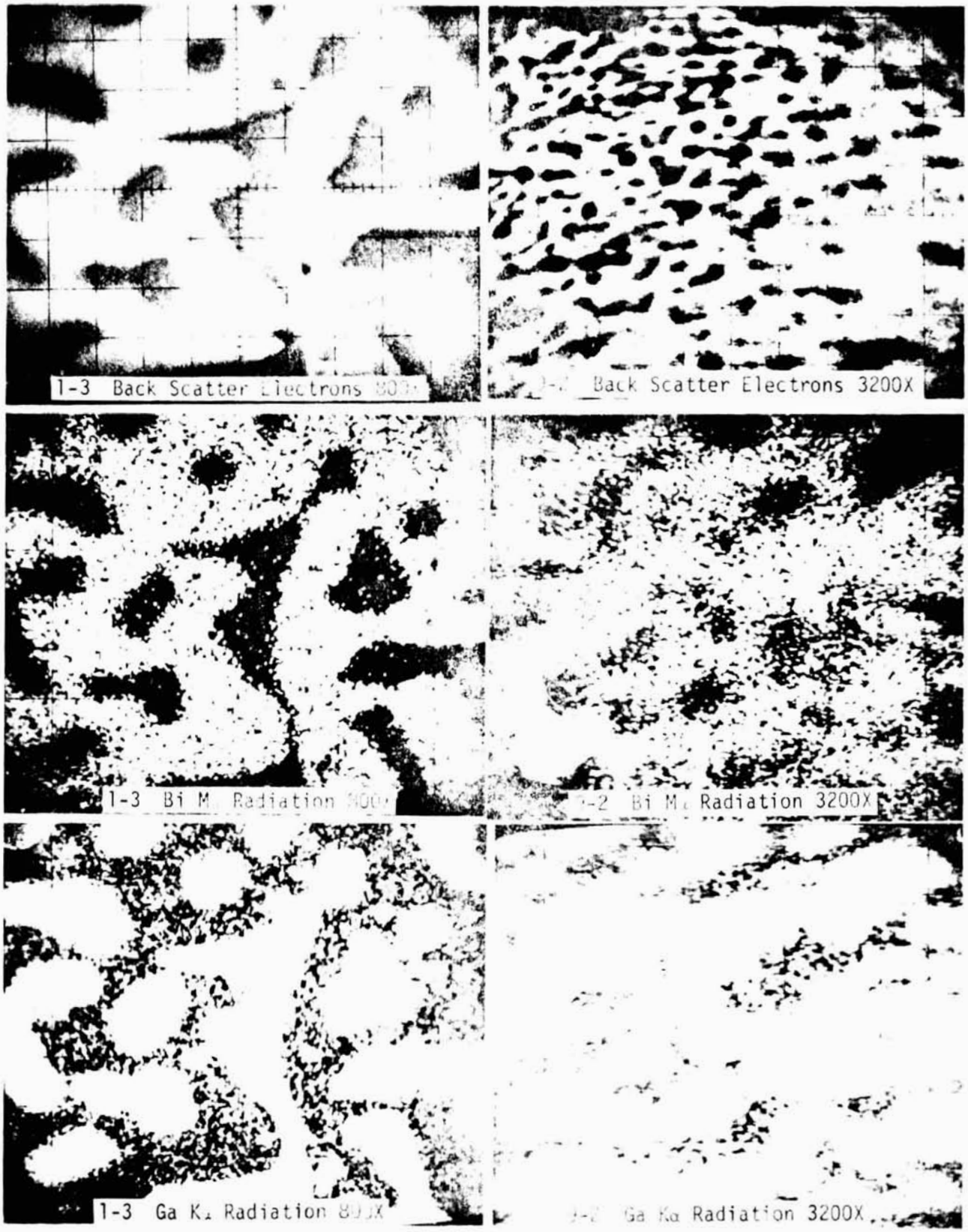

Figure 21. Microprobe Analyses of Specimens 1-3 and 9-2.

TABLE 2

HALL COEFFICIENT, RESISTIVITY, AND HALL MOBILITY IN

Ga-Bi IMMISCIBLE SYSTEMS AT ZERO MAGNETIC FIELD

MATERIAL	HALL COEFFICIENT m^3/C	RESISTIVITY (ROOM TEMPERATURE) ($\mu\Omega$-cm)	RESISTIVITY (-78.5°C) ($\mu\Omega$-cm)	HALL MOBILITY (cm^2/VOLT-SEC)
Ga-Bi SAMPLES:				
1-3 (CONTROL)	-2.5×10^{-7}	57	640	4,400
2-4	-3.4×10^{-7}	69	940	4,900
9-2	-3.8×10^{-7}	91	N/A	4,200
4-5	-1.8×10^{-7}	74	480	2,400
5-6	-5.7×10^{-7}	115	350	5,000
Bi	-11×10^{-7}	123.2		8,980
Ga	-6.3×10^{-11}	17.4		3.62
Bi - 0.5 at. % Ga.	-11×10^{-7} (a)			

(a) LANDOLT-BORSTEIN, 6 Aufl., Bd. II/6, NO CHANGE OBSERVED ON ALLOYING WITH 0.5 at. % Ga.

an increase in effective carriers. Since bismuth is the continuous phase, it probably is largely contributing to the Hall coefficient, with some contribution from the gallium. Since the Hall coefficient is two to seven times smaller than pure polycrystalline bismuth, this indicates that the specimens have two to seven times more carriers than bismuth.

2. The room temperature resistivity values are lower than pure bismuth, which agrees with the postulation of additional carriers as indicated by the Hall coefficient values.

3. The negative temperature coefficient of resistance (TCR) of the specimens, together with the Hall coefficient mobility and resistivity values, is indicative that the system is behaving as a heavily doped semiconductor.

4. The Hall mobility ($\mu = \frac{e\tau}{m}$) is independent of carrier concentration. Thus the decrease in the mobility as contrasted to bismuth may be due to (a) a decrease in the relaxation time τ, or (b) an increase in effective mass m. Most likely it is due to a decrease in relaxation time, resulting in increased surface (in the bulk) scattering from the second phase dispersion of the gallium in the bismuth.

7.2 Superconductivity Measurements

Superconductivity measurements were made on all of the specimens. The method utilized was similar to that of Merriam and Von Herzen [Reference 4] in that each specimen was individually placed in a tuned (1.4 kHz) induction coil and a 33 ohm carbon resistor mounted in thermal contact with the coil. Figure 22 schematically illustrates the instrumentation utilized, and Figures 23 and 24 are photographs of the actual apparatus. When the sample becomes superconducting, the rejection of the magnetic field causes a voltage shift which is detected by the wave analyzer and plotted on an X-Y recorder along with the temperature. An

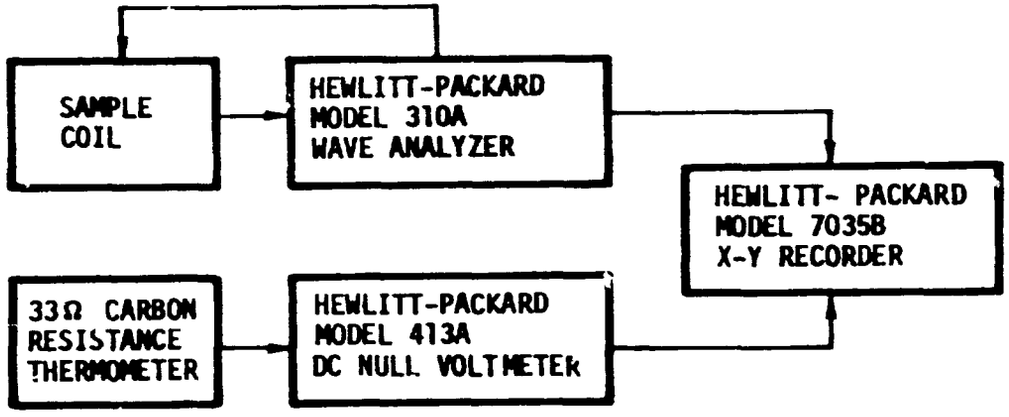

Figure 22. Block Diagram of Superconductivity Apparatus

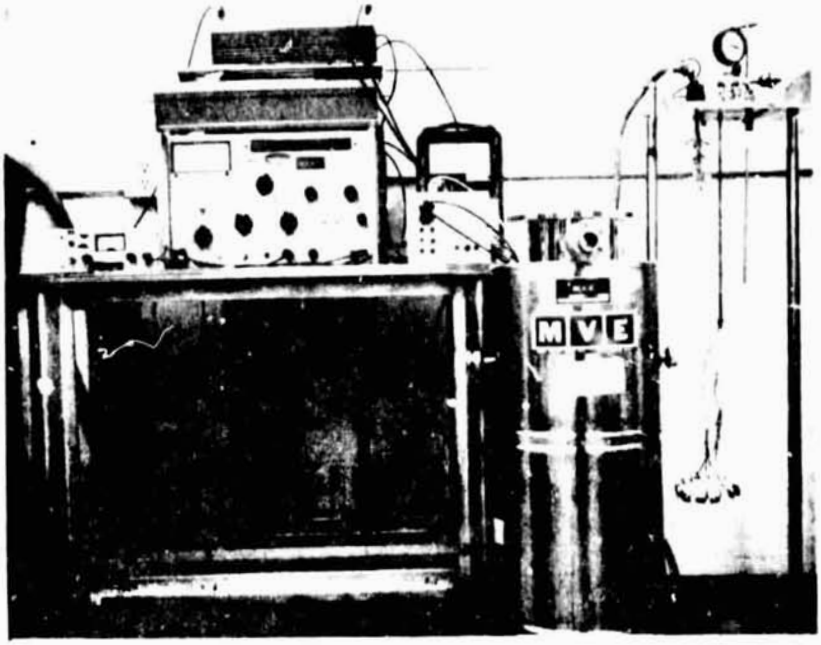

Figure 23. Instrumentation and Apparatus Utilized in the Superconductivity Tests.

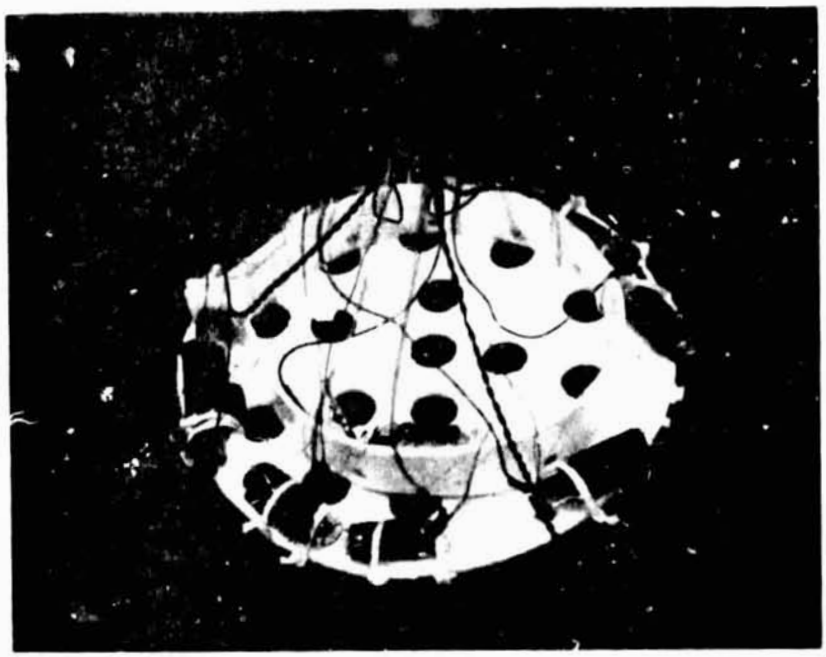

Figure 24. Close-up Photograph of Specimen Coils

additional feature of this method is that multiple transitions can be observed during a single temperature sweep. The temperature of each specimen was measured by recording the voltage drop across the resistor, which was generated by a constant current through the resistor. Power dissipation in the carbon resistance thermometers did not exceed 10 μW. The temperature calibration was done by utilizing a niobium sample, and the unknown temperatures were read from a three point plot of voltage versus temperature on log-log paper through the points 4.2, 9.2 and 297°K for each resistor. The average transition temperatures are considered to be accurate to $\pm$ 0.5°K.

The temperature sweep was obtained by raising and lowering the sample platform containing the samples in the coils through the temperature gradient above the helium level, in a MVE model HLSM-60 cryostat.

Initial experiments were conducted from approximately 1.6°K (lower limit of system) to 4.2°K, and no transitions were apparent in the samples. The experiments were then performed from 4.2°K to approximately 20°K, where superconducting transitions were found. The transition temperature curves for specimens 4-5 and niobium are shown in Figures 25 and 26 which were typical for each specimen except 1-3. The small hysteresis of the curves indicates that good temperature equilibrium was obtained. Table 3 gives the transition temperatures obtained on the samples, plus some reference transition temperatures for various forms of gallium and bismuth.

The T_c values for specimen 2-4 were obtained in a larger coil, with a concomitant smaller signal to noise ratio. The T_c value is probably comparable to the other dropped specimens, but due to coil malfunction during final testing, a value corresponding to the other samples under identical test conditions could not be obtained. Specimen 1-3 showed anomalous behavior in three different coils and under two separate test conditions. The inductance of the final test coil changed continuously from approximately 14°K to 6°K, with sharp change near 7.4°K. Figure 27 is a trace from the final test run, showing this anomalous behavior.

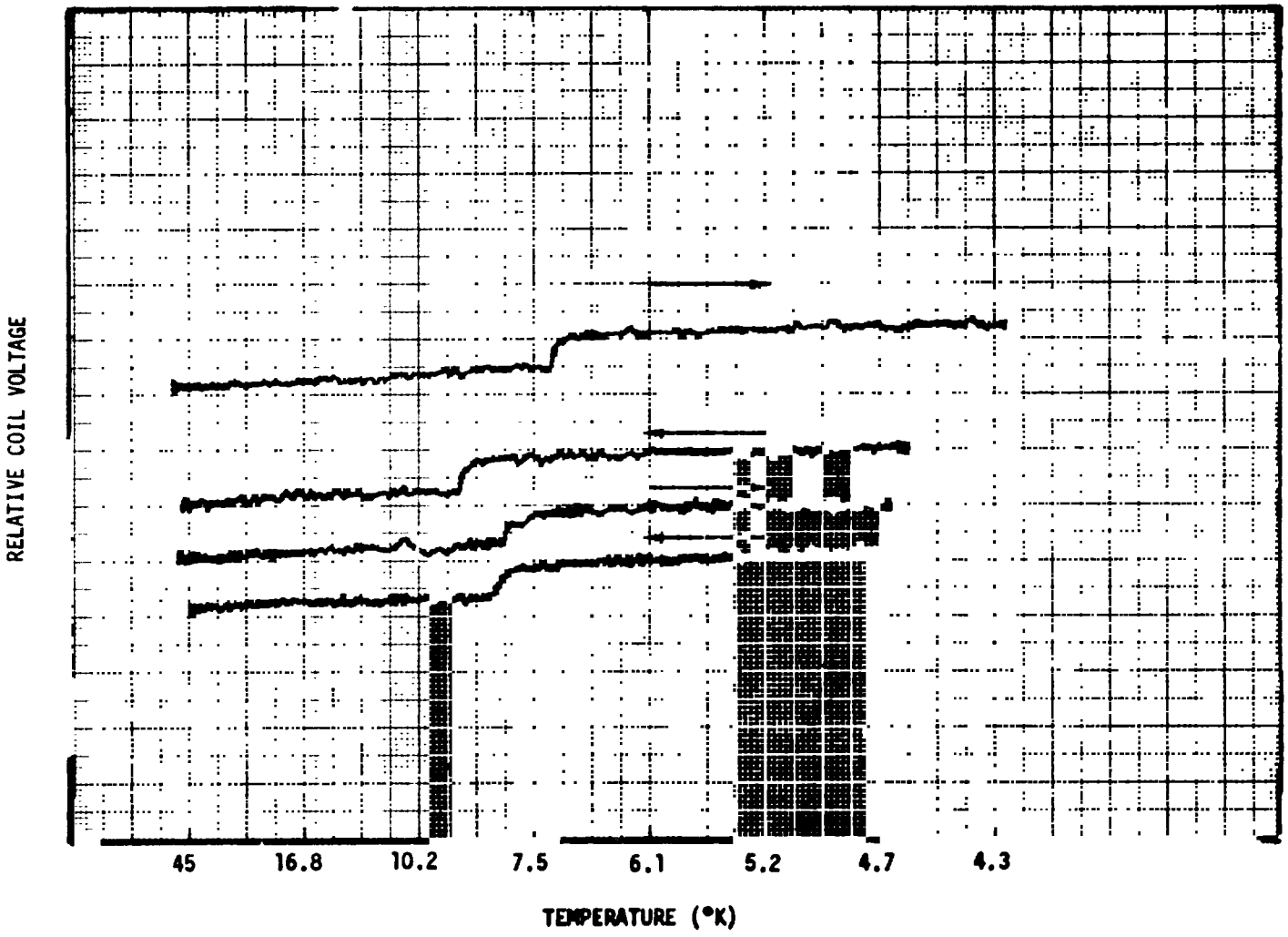

Figure 25. Superconducting Transition in Specimen 4-5
(arrows indicate direction of temperature sweep)

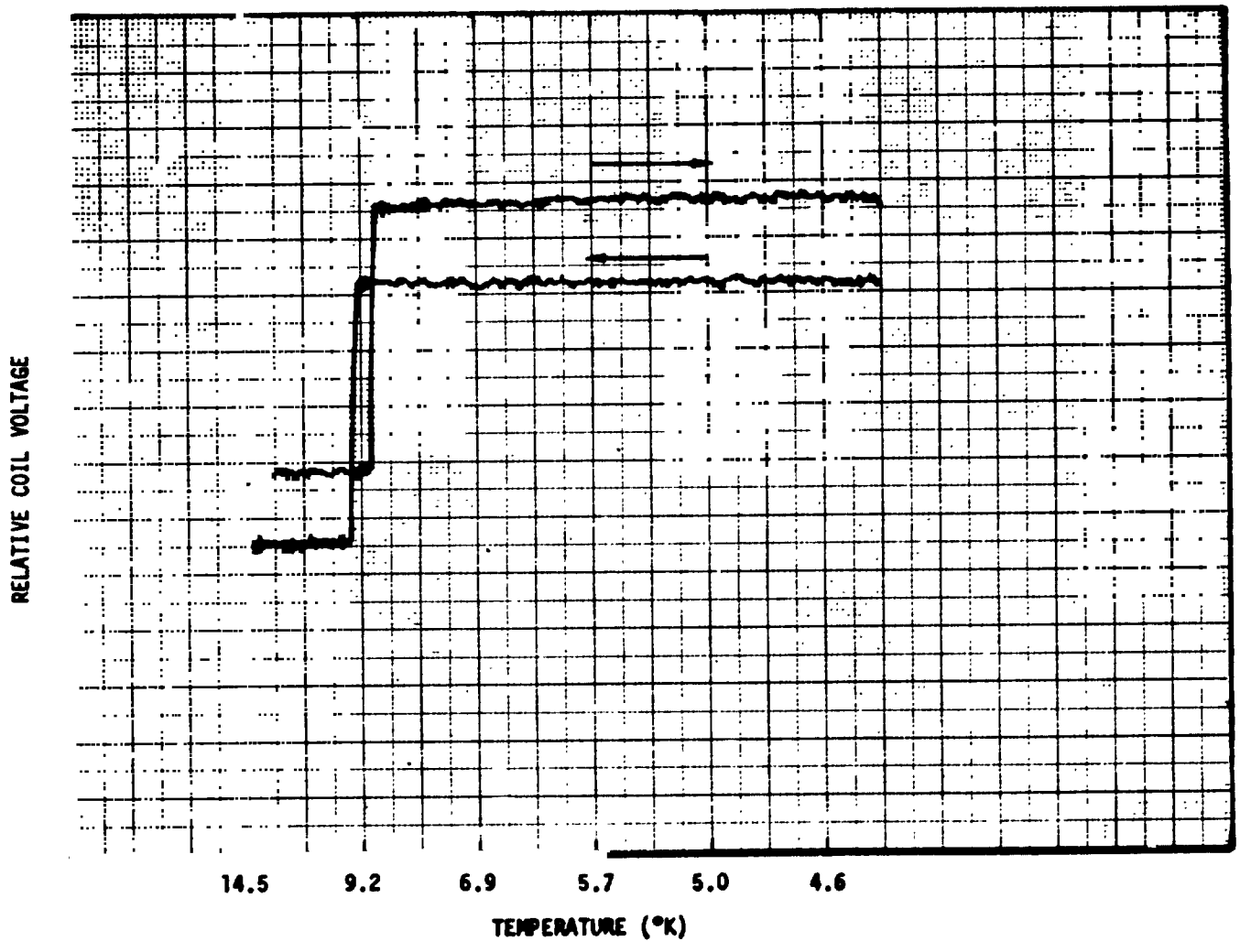

Figure 26. Superconducting Transition of Niobium
(arrows indicate direction of temperature sweep)

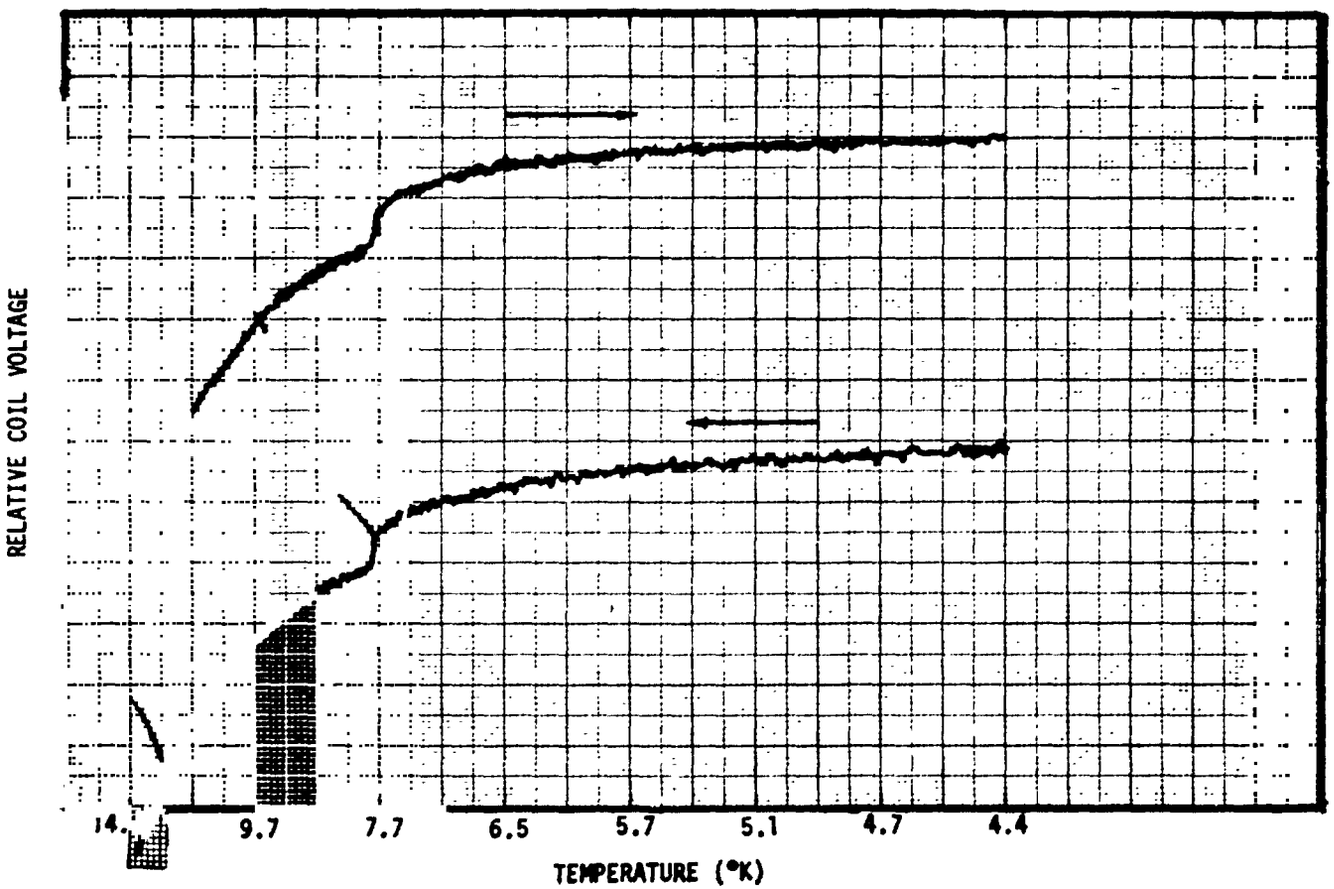

Figure 27. Anomalous Behavior of Specimen 1-3 During Superconductivity Tests (arrows show direction of temperature sweep)

TABLE 3

SUPERCONDUCTIVITY TRANSITION TEMPERATURES
OF GALLIUM-BISMUTH IMMISCIBLE SYSTEMS AND
OTHER FORMS OF GALLIUM AND BISMUTH

MATERIAL	TRANSITION TEMPERATURE (°K)	REFERENCES
Ga-Bi Samples: [a]		
1-3 (Control)	7.4 [b]	
9-2	7.4	
4-5	8.0	
5-6	7.5	
2-4	6.0 [c]	
Literature Values		
Bulk Ga, α phase	1.091	5
Particulate Ga, β phase	6.2	18
Particulate Ga, γ phase	7.6	18
Bulk Ga (unknown modification at 35,000 atm)	6.3	19
Bulk Ga (unknown modification at 35,000 ⟶ 1 atm)	7.5	19
Thin film Ga (formed below 10°K)	8.40	6,8
Thin film Ga (formed at 300°K)	7.2	17
Bulk Bi	not superconducting	7
Bi II (25,000 - 26,800 atm)	∿3.9	10,11,12
Bi III (27,000 - 28,400 atm)	7.2	10,11,12
Thin film Bi (formed below ∿10°K)	∿6	8,9

(a) Midpoint T_c averaged

(b) Possible transition

(c) Results from different coil configuration

It is strongly suggested that this phenomena be investigated further.

The superconducting transition temperatures of the samples are surprising in that bulk bismuth does not superconduct, bulk gallium (α phase) superconducts at approximately 1°K (well below the T_c values obtained), and alloying between gallium and bismuth is negligible. As shown in Table 3 there are anomalous gallium and bismuth phases or modifications which have T_c values close to those obtained in these samples, such as thin film gallium [References 3, 8, 17], particulate β and/or γ gallium [Reference 18], thin film bismuth [References 8 and 9], or high pressure bismuth III [Reference 10, 11 and 12]. Actually, thin film bismuth and bismuth III may be the same phase [Reference 10]. Chester and Jones [Reference 13] suggest that bismuth is nearly a superconductor and the transition in bismuth III is associated with a transition to a more closely packed crystalline form. Merriam and Von Herzen [Reference 4] have obtained increased T_c values from quenched In-Sn alloys and Sn-Ga (mutually insoluble in the solid-state) mixtures due to induced plastic strains. Another source of the higher T_c values could be from the large surfaces of the gallium and bismuth acting as "granular superconducting" material [References 14, 15 and 16] in which small grains (20-200Å) have much higher T_c values.

Thus there are several explanations for the T_c values obtained: (a) anomalous phases of gallium and/or bismuth present in the bulk, (b) anomalous phases between the internal surfaces of the dispersed gallium and bismuth, (c) large internal pressures exerted on the bulk materials during solidification, resulting in plastic deformation in the specimens, or (d) a combination of the above three.

A simplified stress analysis was performed to determine if the expansion of gallium and bismuth during solidification could produce relatively high internal stresses within the samples. The assumption was made that a sphere of gallium was embedded in bismuth, and that a radial stress was caused by (1) the expansion of gallium alone, and (2) both the expansion of bismuth and gallium. Gallium has a volume expansion of 3.1% [Reference 20] and bismuth has a volume expansion of

3.3% [Reference 21]. The mechanical properties of gallium could not be found, therefore the properties of bismuth were utilized [Reference 21] as an approximation.

The calculated radial stresses gave a range of values between 10^3 MPa (10,000 atm) and 10^4 MPa (100,000 atm), depending upon the degree of expansion. Comparison of these values with those of Zharkov and Kalinin [Reference 23] for antimony and other metals that should be similar to gallium suggest that a value of approximately 5×10^3 MPa (50,000 atm) is qualitatively accurate. These values bracket the pressure ranges for Bi II and Bi III. In addition, Buckel and Gey [Reference 19] observed that gallium superconducts at 6.3°K at 3.5×10^3 MPa (35,000 atm) and upon lowering the pressure to 0.1 MPa (1 atm), the T_c was raised to 7.5°K without an apparent phase transition. By comparison, Feder, et.al. [Reference 18] prepared their samples by ultrasonically dispersing gallium at 50°C in an ethyl alcohol/sodium oleate solution and cooling the dispersed specimens by two different methods. The first method consisted of cooling to room temperature, then quenched in liquid nitrogen and brought to liquid helium temperature. This produced both β and γ gallium in a 5:1 ratio respectively as measured by frequency shift during a temperature sweep (experimental method similar to the one used in this program). The second method consisted of quenching to 0°C and holding the specimen at that temperature for 24 hours before cooling to liquid helium temperatures. This method produced α and β gallium in the ratio of 4:1, with a very small amount of γ gallium.

The crystallographic cell constants of β and γ gallium are not given in the standard X-ray files [Reference 22], and Reference 18 did not give the details of their X-ray study done at liquid nitrogen temperatures. Thus a comparison cannot be made between the various authors referenced and the specimens processed at MSFC.

As mentioned previously, the T_c values given in Table 3 are averaged and comparison of Figure 25 for specimen 4-5 with Figure 26 for niobium shows that the transition for 4-5, while clear, is somewhat more diffuse than the niobium transition. Since the apparatus is capable

of detecting multiple T_c's, it appears that the total transition involves both bismuth and gallium.

Inasmuch as the gallium is finely dispersed in the bismuth, it may be exhibiting the "granular superconducting" effect [References 14, 15 and 16] or acting as a thin film as well [Reference 17], since a large number of the gallium particle sizes are within this size regime.

The main transition, however, probably is due to pressure effects (e.g., γ Ga and Bi III), as evidenced from the metallurgical examination and stress calculations. This is corroborated by the slight slope to the curves near the main transition point, since the internal pressure and consequently the transition point(s) [Reference 4] will vary with temperature due to change in thermal expansion. The unusual behavior of specimen 1-3 may also be due to this effect, although the curve is so anomalous that other unknown factors must be contributing also. Since most of the high T_c forms of gallium and bismuth lie within the transition region of the specimens, it is difficult to pinpoint precisely the exact superconducting mechanism that is occurring.

8.0 CONCLUSIONS

The experimental drop tower package, designed to solidify heated specimens during the four second, low gravity free fall conditions, operated satisfactorily and met all the test criteria.

Stable dispersions of gallium in bismuth were successfully processed in the MSFC drop tower facility utilizing the experimental drop tower package.

Metallurgical examination of both the control and low gravity processed specimens included optical and scanning electron microscopy and electron microprobe analyses. Each of these methods demonstrated that the microstructure of the low gravity processed specimens exhibited a finer and more even dispersion of gallium in bismuth than the one gravity control specimen. The majority of dispersions of gallium in the low gravity processed specimens were 1 μm or less. From an estimation of the available time before the monotectic bismuth solidification temperature was reached, and calculation of the Rayleigh number for the gallium-bismuth system, thermal convection cells could be set up in the sample container which would give the microstructure seen in the control specimen. The calculated Froude number was less than unity, thus no unusual sedimentation effects were observed.

The metallurgical examination also indicated the following:

1. The cooling rate appears to have a definite effect on dispersion size, with slower cooling rates giving finer dispersions.

2. The expansion of both bismuth and gallium upon solidification appears to have affected the microstructure, particularly the low gravity processed specimens. The effect is primarily manifested by the appearance of "grain boundaries" which upon closer examination were found to be filled with gallium.

3. Although the dispersion in the low gravity processed samples was too fine to permit a complete electron microprobe analysis, traces on the control sample showed little or no alloying between the gallium and bismuth.

Measurement of the Hall voltages and bulk resistivities of the samples gave the following results:

1. The Hall coefficients are two to seven times smaller than the values for pure polycrystalline bismuth. Since bismuth is the continuous phase, the carrier concentration in the processed samples is two to seven times larger. The type of carriers (electrons or holes) could not be determined since the conventional method would destroy the samples.

2. The decrease in Hall mobility from that of bismuth is probably attributable to a decrease in the relaxation time due to bulk carrier scattering by the dispersed gallium.

3. The lower room temperature resistivity values as compared to bismuth are indicative of additional carriers and corroborate the Hall mobility results.

4. The negative temperature coefficient of resistance, along with (2) and (3) show that all of the specimens, including the control specimen, are behaving as heavily doped extrinsic semiconductors.

Superconductivity tests on the processed specimens were performed from approximately 1.6°K to 20°K. The majority of the low gravity processed specimens superconducted between 7.4 to 8.0°K, with an uncertainty of $\pm$ 0.5°K. One of the low gravity processed samples (2-4) superconducted at 6.0°K; however, this was an earlier test with a different coil configuration and may not be indicative of the true transition

temperature.

The control specimen (1-3) showed a very anomalous behavior in terms of a superconducting transition point. There may be a possible transition point at 7.4°K, but it is strongly suggested that this sample be investigated further.

Investigation into the superconducting mechanisms that may be occurring did not reveal the exact mode, but the following is postulated:

1. High internal pressures and plastic strains probably exist in the specimens. This is corroborated by a stress analysis and could give rise to the higher transition forms of gallium (γ gallium) and/or bismuth (bismuth III). The slight change in slope in the transition curves as the temperature is changed also tends to confirm the pressure/strain effect.

2. The extremely fine dispersion of gallium in bismuth may also give rise to the "granular superconducting" effect. Also, a film effect may be present due to the large internal gallium/bismuth interface surfaces that exist in the low gravity processed specimens.

9.0 REFERENCES

1. "Space Processing and Manufacturing," ME-69-1, Conference at MSFC, October 21, 1969, p. 183.

2. Apollo Experiment Definition Study, November 1971, Final Report, Phase II, NASA Contract NAS 8-27085, TRW Systems Group Report No. 18677-6009-RO-00.

3. Test and Evaluation of Apollo 14 Composite Casting Demonstration Specimens 6, 9 and 12, September 1971, Final Report, Phase I, NASA Contract NAS 8-27085, TRW Systems Group Report No. 18677-6006-RO-00.

4. M. F. Merriam and M. Von Herzen, "Superconductivity in the Indium-Tin System," Phys. Rev. 131, 637 (1963).

5. J. F. Cochran and D. E. Mapother, "Superconducting Transition in Zinc and Gallium," Phys. Rev. 121, 1688 (1961).

6. W. Buckel, International Conference on Low Temperature Physics and Chemistry, Madison, Wisconsin (1958), p. 326.

7. B. W. Roberts, "Superconductive Materials and Some of Their Properties," in Progress in Cryogenics, Vol. 4, K. Mendelssohn, ed., Academic Press, New York, (1964).

8. R. Hilsch and W. Maritanssen, "Gitterstörungen in Dünnen Schlichten," Nuovo Cim. Suppl. 7, 480 (1958).

9. F. Reif and M. A. Woolf, "Energy Gap in Superconductors Containing Paramagnetic Impurities," Phys. Rev. Letters 9, 315 (1962).

10. N. B. Brandt and N. I. Ginzburg, "Superconductivity of Crystalline Modifications of Bismuth," Soviet Physics JETP 12, 1082 (1961).

11. N. B. Brandt and N. I. Ginzburg, "Investigation of Crystalline Modifications of Bi and Certain Questions in the Method of Obtaining High Pressure at Low Temperatures," Soviet Physics Solid State 3, 2510 (1962).

12. N. B. Brandt and N. I. Ginzburg, "Critical Fields of the Crystal Modifications Bi II and Bi III," Soviet Physics JETP 17, 326 (1963).

13. P. F. Chester and G. O. Jones, Phil Mag. 44, 1281 (1953).

14. R. W. Cohen and B. Abeles, Phys. Rev. 168, 444 (1968).

15. J. H. P. Watson, Appl. Phys. Letters 15, 125 (1969).

16. J. Hurault, J. Phys. Chem. Solids 29, 1765 (1968).

17. B. Abeles, R. W. Cohen and G. W. Cullen, Phys. Rev. Letters, 17, 632 (1966).

18. J. Feder, S. R. Kiser, F. Rothwarf, J. P. Burger and C. Valette, Solid State Commun., 4, 611 (1966).

19. W. Buckel and W. Gey, Physik, 176, 336 (1963).

20. R. N. Lyon, Ed., Liquid Metals Handbook, NAVEXOS P-733 (Rev.), Joint Publication of the Atomic Energy Commission and Department of Navy, Washington, D. C., June 1952.

21. C. A. Hampel, Ed., Rare Metals Handbook, Reinhold Pub. Corp., N.Y., N.Y., 2nd Ed., 1961.

22. L. G. Berry, Ed., Inorganic Index to the Powder Diffraction File 1971, Publication PDIS-2II, Joint Committee on Powder Diffraction Standards, Swarthmore, Pennsylania 19081.

23. V. H. Zharkov and V. A. Kalinin, Equations of State at High Pressures and Temperatures, Consultants Bureau, N.Y., N.Y., 1969.

☆U.S. GOVERNMENT PRINTING OFFICE 1976—641-255/573 REGION NO. 4